Computing Sextic Centrifugal Distortion Constants by DFT: a Benchmark Analysis on Halogenated Compounds

Andrea Pietropolli Charmet[a,§], Paolo Stoppa[a], Nicola Tasinato[b], Santi Giorgianni[a]

[a]*Dipartimento di Scienze Molecolari e Nanosistemi, Università Ca' Foscari Venezia, Via Torino 155, 30172 Mestre (VE), Italy*

[b]*Scuola Normale Superiore, Piazza dei Cavalieri 7, 56126 Pisa (Pi), Italy*

Abstract

This work presents a benchmark study on the calculation of the sextic centrifugal distortion constants employing cubic force fields computed by means of density functional theory (DFT). For a set of semi-rigid halogenated organic compounds several functionals (B2PLYP, B3LYP, B3PW91, M06, M06-2X, O3LYP, X3LYP, ωB97XD, CAM-B3LYP, LC-ωPBE, PBE0, B97-1 and B97-D) were used for computing the sextic centrifugal distortion constants.The effects related to the size of basis sets and the performances of hybrid approaches, where the harmonic data obtained at higher level of electronic correlation are coupled with cubic force constants yielded by DFT functionals, are presented and discussed. The predicted values were compared to both the available data published in the literature and those obtained by calculations carried out at increasing level of electronic correlation: Hartree-Fock Self Consistent Field (HF-SCF), second order Møller-Plesset perturbation theory (MP2), and coupled-cluster single and double(CCSD)level of theory.Different hybrid approaches, having the cubic force field computed at DFT level of theory coupled to harmonic data computed at increasing level of electronic correlation (up to CCSD level of theory augmented by a perturbational estimate of the effects of connected triple excitations, CCSD(T)) were considered. The obtained results demonstrate that they can represent a reliable and computationally affordable method to predict sextic centrifugal terms with an accuracy almost comparable to that yielded by the more expensive anharmonic force fields fully computed at MP2 and CCSD levels of theory. In view of their reduced computational cost, these hybrid approaches pave the route to the study of more complex systems.

KEYWORDS: DFT functionals; anharmonic force fields; sextic centrifugal distortion constants.

[§]Corresponding author: jacpnike@unive.it; Phone: +39 041 2348541
Address: Universita' Ca' Foscari Venezia, Dipartimento di Scienze Molecolari e Nanosistemi Via Torino 155, 30172 Mestre (VE)– (Italy)

1.Introduction

It is nowadays widely recognized the importance of molecular spectroscopy in providing data with the accuracy needed for detailed structural investigations. Anyway, the analysis of spectroscopic measurements, especially for larger systems, is often a very complex and time-consuming task. For this reason, in the last decade, the experimental investigations were increasingly coupled to computational studies, since the latter are able to provide reliable predictions of several parameters which, in turn, can be employed to simulate the spectra. On the other hand, the experimental data can be used to benchmark the theoretical predictions of the different available computational strategies [1]. Given this fruitful interplay of theory and experiment it is therefore highly desirable to investigate the properties like accuracy and convergence behaviors of the different computed values. Within the framework of vibrational perturbation theory up to the second order (VPT2) [2–4], many spectroscopic parameters can be obtained from the anharmonic force field data. For calculating the properties relevant to rotational spectroscopy (e.g. vibrational corrections to equilibrium rotational constants and sextic centrifugal distortion constants), the cubic force constants are often needed.

Concerning the computations of rotational constants, there is a remarkable amount of literature studies focused on their dependence on the level of theory and basis set (see for example Refs. [5–7] and references therein). The derivation of accurate equilibrium structure by means of *ab initio* computed corrections to the experimental ground-state rotational constants were also extensively investigated (see, for example, Refs. [8–11] and references therein). Nowadays the methods of choice for accurately computing the vibrational corrections are those based on high level of electronic correlation, and the coupled cluster level of theory with single and double excitations augmented by a perturbational estimate of the effects of connected triple excitations, CCSD(T) [12-14], is considered the "*gold standard*" for this task [15–17]. The downside of this approach lies in its unfavorable scaling with respect to the system size, that limits the applicability to molecules having not more than ten atoms. Recently the performances of the hybrid functional B3LYP [18-21]were positively reviewed [10, 11] in view of its satisfactory results with less demanding computational cost. Actually, approaches based on density functional theory (DFT) were proved to perform very well for calculations of anharmonic corrections to vibrational properties [22–24], especially when coupled to harmonic data yielded by computations carried out at CCSD(T) level of theory [25–27]. Their predictions of anharmonic corrections to intensities and of the coupling parameters for interacting vibrational states are comparable (or even better) to those obtained at second order Møller-Plesset perturbation theory, MP2 [28], and even at coupled cluster level of

theory. Anyway, to the best of our knowledge, the performances of DFT functionals in yielding reliable sextic centrifugal distortion constants have not thoroughly investigated so far. In the present work we therefore carried out a systematic study on the use of DFT methods to predict these data; several functionals were employed to compute the cubic force constants using the correlation consistent Dunning's basis set [29–31] cc-pV*n*Z (*n* = D,T and Q) and their augmented diffuse counterparts, aug-cc-pV*n*Z. Additional calculations were carried out by using the B3LYP functional in conjunction with the SNSD [25, 32] and N07D [32] basis sets. We performed the investigation on a set of four small semi-rigid molecules, focusing on halomethanes and haloethenes, a class of compounds which in recent years was the subjects of several theoretical and experimental investigations (see for examples Refs. [33–48] and references therein). For these molecules very accurate computed values are available in literature (i.e. obtained from calculations performed at CCSD(T) level of theory with at least triple-ζ basis set). These values were taken as reference data in the current work to benchmark the DFT methods, which are computationally much less demanding and therefore applicable to the study of larger systems. It is worthwhile to note that some of their experimentally obtained sextic constants are not well determined (being strongly correlated and affected by errors rather large). Concerning the halomethanes, because of their atmospheric relevance we chose difluoromethane, CH_2F_2, and chlorofluoromethane, CH_2ClF; for both of them very accurate *ab initio* predictions and experimental data coming from previous studies are available (see for example Refs. [49–51] for CH_2F_2 and Refs. [26, 52, 53] for CH_2ClF). As haloethenes, we chose 1-chloro-1-fluoroethene, $ClFC=CH_2$, and chlorotrifluoroethene, $F_2C=CFCl$, since they can be considered representative of X-C=C-Y systems, where the C atoms, sp^2 hybridized, are linked to X and Y atoms; besides, they are potential trace gas pollutants. For these reasons, in recent years both of them were the subjects of several experimental and theoretical investigation; see, for example Refs. [27,54–57] for $ClFC=CH_2$ and Refs. [58–63] for $F_2C=CFCl$.

In total, we used 13 functionals: eight hybrids (B3LYP, B3PW91 [64, 65], PBE0 [66], O3LYP [67], X3LYP [68], M06, M06-2X[69], and B97-1 [70]), three range-separated (CAM-B3LYP [71], LC-ωPBE [72–74], ωB97XD [75]), one GGA (B97-D [76]), and the double-hybrid B2PLYP [77]. Their convergence behaviors with respect to the basis sets employed were analyzed, and the comparison with the corresponding results obtained using different increasing levels of electron correlation (HF, MP2 and CCSD) allowed us to assess their overall performances. In addition, we worked out different hybrid force fields where the harmonic data, obtained at higher level of electronic correlation like CCSD and CCSD(T), were coupled to the cubic force constants yielded by DFT methods; their performances were compared with those achieved by hybrids having the harmonic data calculated at B2PLYP level of theory.

2. Methodology and computational procedure

In all the quantum chemical calculations described in the present work, we first optimized the molecular geometry and then we computed the harmonic force field. In a subsequent step, we evaluated the cubic force constants by carrying out the numerical differentiation of the analytical hessians computed at points displaced along the normal coordinates, following the procedure described by Schneider and Thiel [78]. By using these cubic force constants, expressed in dimensionless normal coordinates, in conjunction with the equilibrium rotational constants, the inertial derivatives and the Coriolis coupling constants, we computed the sextic centrifugal distortion constants employing the expressions available in the literature [79–81]. Being all the molecules considered in the present work asymmetric rotors, among the Hamiltonian reduction mostly used [81, 82] we employed the Watson's A-reduction for CH_2F_2, CH_2ClF and $ClFC{=}CH_2$, and the Watson's S-reduction for $F_2C{=}CFCl$.

We performed all the calculations of the analytical hessians by using two different suites of program packages: Gaussian09 [83] for DFT, HF and MP2 computations, and CFOUR [84] for those carried out at CCSD level of theory. For all the density functionals employed, we used the option *UltraFine* grid available in Gaussian09 (corresponding to 99 radial and 590 angular points), given its good results (see for example Refs. [27, 85]) for anharmonic force field computations. At DFT and MP2 levels of theory, we used the Dunning's correlation-consistent cc-pV*n*Z and aug-cc-pV*n*Z basis sets, with n = D, T and Q (for CH_2F_2 and CH_2ClF we carried out the calculations at HF-SCF and MP2 levels extending the basis set up to cc-pV5Z). These basis sets, for brevity, are labeled as V*n*Z and AV*n*Z, respectively. For the computations carried out on haloethenes, to avoid the known problems [25] related to low accuracy when using diffuse functions on all the atoms, we used the augmented aug-cc-pVTZ and aug-cc-pVQZ basis sets only on fluorine atoms: in the present work these basis sets are referred to as VTZ-AVTZ(F) and VQZ-AVQZ(F), respectively.

3. Results and discussion

3.1 Results obtained at HF-SCF, MP2 and CCSD levels of theory

First of all, we investigated the convergence of the values of the sextic centrifugal distortion constants obtained at both HF-SCF and MP2 level of theory in conjunction with the hierarchical series of basis sets V*n*Z, ranging from double- to quintuple-zeta quality, taking CH_2F_2 and CH_2ClF as test molecules (the results obtained at HF-SCF and MP2 levels of theory are available as Supplementary Material for this article, see Tables S1 and S2).

Going from triple-zeta to larger basis sets both methods show a monotonic trend for each constant, even if not the same for all constants. At HF-SCF level of theory, considering for example CH_2F_2, going from triple-zeta to quintuple-zeta some of the sextic centrifugal distortion constants increase while the others decrease, and the same behavior happens for CH_2ClF. Looking at the effects related to the basis set size we estimate that, on average, at HF-SCF level of theory when using the V5Z basis set the errors due to basis-set truncation could be considered almost negligible. Focusing on the results obtained at the MP2 level of theory we note that the use of the V5Z basis set yields values having almost negligible errors due to basis-set truncation. The results reported suggest also that the AVTZ basis set could provide sufficiently accurate estimates of the corresponding CBS limit values, differing on average less than 3% with respect to that obtained with the use of V5Z basis set.

Then, we analyzed the effect of increasing the level of electron correlation by performing calculations at HF-SCF, MP2 and CCSD level of theory and using the VTZ basis set augmented by diffuse functions for halomethanes, while for haloethenes we used the augmented cc-pVTZ basis set only for fluorine atoms. We previously demonstrated how this kind of basis set is well suited for anharmonic computation on haloethenes [27]. It is worthwhile to point out that CCSD calculations perform remarkably well with respect to the reference data. From the analysis of the overall results (data available as Supplementary Material for this article, see Tables S3 and S4) we conclude that, provided the use of a basis set at least of triple-ζ quality, CCSD level of theory yields sextic centrifugal distortion constants in very good agreement with respect to the ones computed at CCSD(T) level, thus confirming the previous findings for $HD^{17}O$ [86]. With respect to CCSD data, in conjunction with triple-zeta basis set, the data suggest that the MP2 level of theory can be employed as alternative to CCSD computations, being computationally less demanding, while even the HF-SCF method can be used to have satisfactory estimates.

3.2 Results obtained at DFT level for halomethanes

For CH_2F_2 and CH_2ClF we investigated the convergence behavior of the sextic centrifugal distortion constants computed by means of DFT methods by using correlation consistent basis sets V*n*Z with *n*= D, T and Q, and their augmented counterparts, AV*n*Z, for analyzing the effects of adding diffuse functions. In addition, we checked the performance of basis sets having diffuse functions only on fluorine atoms, labeled as V*n*Z-AV*n*Z(F), *n* = D, T and Q. On average, the differences between the results obtained in conjunction with AVTZ basis set and those given by the use of VTZ-AVTZ(F) can be considered almost negligible. The same holds when considering the differences between the values obtained in conjunction with AVQZ and VQZ-AVQZ(F) basis sets

(as an example of the trends generally observed, in Table S5 of the Supplementary Material for this article we report the results for B3LYP functional).

We evaluated the performances of the different combinations of functionals and basis sets by computing the MAD and the maximum absolute percentage deviation, MAX, from the computed values available in the literature for both the molecules. Table 1 lists the results obtained for CH_2F_2, while Table 2 reports those found for CH_2ClF.

Concerning the results obtained for difluoromethane (see Table 1), we note that employing the AVQZ basis sets the best performances (in terms of mean absolute deviation with respect to the best computed data) are given by PBE0 with MAD equals to 1.5%, followed by ωB97XD, M06-2X, CAM-B3LYP and B97-1. When moving to the AVTZ basis set, the best five DFT models are LC-ωPBE, M06-2X, PBE0, ωB97XD and CAM-B3LYP. The basis set dependence of the performances of the different functionals is illustrated in Figure 1, where the corresponding results (MAD with respect to the best computed data reported in literature) are shown. We can observe that, on average, going from the AVDZ basis set to AVTZ improves results more than going from AVTZ to AVQZ.

Moving to the chlorofluoromethane (see Table 2), in conjunction with the AVQZ basis set, CAM-B3LYP with MAD equals to 2.5% is the best functional, followed by LC-ω, ωB97XD, PBE0 and B97-1. Going to the AVTZ basis set, ωB97XD, M06-2X and LC-ωPBE have the lowest MAD (2.4%), followed by CAM-B3LYP, B2PLYP and PBE0. Again, the worst results are obtained by means of B97-D and M06 functionals. Figure 2 shows the basis set dependence of the performances of the different functionals, where the corresponding results (MAD with respect to the best computed data reported in literature) are shown. In this case, going from AVDZ to AVTZ or from AVTZ to AVQZ leads to erratic behavior; anyway, on average, the AVTZ basis set yields good results.

3.3 Results obtained at DFT level of theory for haloethenes

Focusing on $ClFC=CH_2$, we first investigated the performances yielded by the different functionals employing correlation consistent basis sets from VDZ up to VQZ and their augmented counterparts having the diffuse functions only on F atoms. The results are reported in Table 3. By inspection of the statistics (MADs and MAXs), we note that, on average, moving from VTZ-AVTZ(F) to VQZ (or to VQZ-AVQZ(F)) does not lead to relevant improvements, being the differences between the corresponding MAD*s* generally not greater than 1.0% and those between the corresponding MAX*s* on average lower than 2%. At VTZ-AVTZ(F) levels the best results are

yielded by B3PW91 (MAD = 1.3%), PBE0, B97-1, followed by LC-ωPBE and B2PLYP. Among the worst ones we find M06-2X and B97-D; the latter has also the greatest MAX.

Since we did not observe a significant improvement going from triple-zeta to quadruple-zeta basis sets, and taking also into account the corresponding not negligible increase in computational costs due to the use of larger basis set, we carried out the calculations for chlorotrifluoroethene in conjunction only with double- and triple-zeta basis sets. The results obtained for F_2C=CFCl are listed in Table 4. By employing the VTZ-AVTZ(F) basis set the best results are yielded by B3LYP (MAD = 2.6%), followed by X3LYP and B2PLYP. B97-1 and LC-ωPBE have the same MAD, but the latter shows larger deviations, also greater than those found for another range-separated functional, CAM-B3LYP. It is worthwhile to note that the worst results are yielded by ωB97XD, M06 and B97-D.

From the analyses carried out on both molecules, we can conclude that, in conjunction with a basis set of triple-zeta quality, the great majority of the functionals considered lead to satisfactory results (with the exception of B97-D). We can identify as valid alternative to the more demanding CCSD approaches, the B97-1 functional while, among the hybrid ones, we suggest the B3LYP, B3PW91 and PBE0 methods.

3.4 Results obtained by means of hybrid force fields

Taking CH_2ClF as test molecule, we checked the performances offered by hybrid force fields, where the harmonic data computed at CCSD and CCSD(T) levels of theory are coupled to the cubic force constants calculated by DFT methods (we labeled these two sets as CCSD/DFT and CCSD(T)/DFT, respectively); besides, we compared these results with those yielded by employing the cubic data obtained at HF-SCF and MP2 levels of theory. For all these computations we employed the AVTZ basis set. We carried out also hybrid force fields having the harmonic data at B2PLYP/AVTZ level and the cubic ones yielded by B3LYP (this set was labeled as B2PLYP/B3LYP) in conjunction with the SNSD and N07D basis sets.

First, we carried out the CCSD/DFT hybrid force fields in conjunction with the AVTZ basis set. We compared their results with respect to the values computed at CCSD/AVTZ level of theory (which yields values in good agreement with the best computed data); Figure 3 lists the corresponding performances. Focusing on those having the cubic force constants given by DFT models, we see that the best results are obtained by using B97-1, followed by CAM-B3LYP, PBE0, B3PW91 and B2PLYP. Using HF-SCF for computing the cubic part yields a MAD of 4.6%, while the MP2 method, computationally more demanding, leads to a MAD of 2.0%. Among the functionals, the worst are LC-ωPBE, M06 and B97-D (MAD = 6.3%, MAX = 18.6%). For

comparison, the hybrid models having the harmonic data computed at B2PLYP/AVTZ level give a MAD of 6.5% when the cubic force constants are obtained at B3LYP/SNSD level and a MAD of 6.1% when the cubic force constants are calculated at B3LYP/N07D level.

Then, we performed the another set of hybrid force fields, CCSD(T)/DFT, again in conjunction with the AVTZ basis set. Figure 4 shows the corresponding performances with respect to the data obtained by cubic force field obtained at CCSD(T)/AVTZ level. The best agreement is yielded by CAM-B3LYP, then by B3PW91, followed by B2PLYP, B97-1 and O3LYP (MAD = 1.7%). It is worthwhile to note that computing the cubic part at HF-SCF level of theory yields a MAD of 3.9%, while the MP2 method gives a MAD of 2.6%. Among the worst functionals we note LC-ωPBE (MAD= 6.1%, MAX= 14.2%). For comparison, the B2PLYP/B3LYP model yields a MAD of 4.3% when B3LYP is coupled to the SNSD basis set and a MAD of 3.8% when coupled to the N07D one.

We then compared the performances of the different hybrid force fields, CCSD/DFT and CCSD(T)/DFT, with respect to the best computed data reported in the literature (their results are reported as Supplementary Material available for this article, Tables S6 and S7). Figure 5 illustrates the performances of former: among the different functionals B97-1 is the best one, followed by ωB97XD, M06-2X, PBE0 and CAM-B3LYP. Figure 6 illustrates the performances of the CCSD(T)/DFT set: PBE0 and B97-1 are the best ones, followed by CAM-B3LYP, B3PW91 and B2PLYP.

The excellent results yielded by CCSD(T)/DFT hybrid force fields for CH_2ClF stimulated us to check the performances of similar approaches for haloethenes, choosing $ClFC=CH_2$ as test molecules. We therefore coupled the harmonic data computed at CCSD(T) level of theory with the cubic force constants obtained by the several functionals considered in the present work in conjunction with the VTZ-AVTZ(F) basis set. As shown in Figure 7, the best agreement with the best computed data in the literature is given by B3PW91 (MAD = 1.1%), followed by PBE0, CAM-B3LYP and B2PLYP, and then by B3LYP. Considering the overall obtained by the CCSD(T)/DFT sets for both CH_2ClF and $ClFC=CH_2$, the best results are given by B3PW91 functional, followed by CAM-B3LYP, B2PLYP, PBE0 and B97-1.

The good results achieved by using these hybrid approaches prompted us to verify the performances offered by computationally less demanding methods having the harmonic parts computed at B2PLYP levels, which are applicable to larger systems. Again, we focused on CH_2ClF and $ClFC=CH_2$ molecules, employing the B2PLYP functional to compute the quadratic force field in conjunction with the AVTZ basis set (for $ClFC=CH_2$ we employed the VTZ-AVTZ(F) one), while the cubic part is obtained by other DFT methods; these hybrid force fields are referred to as B2PLYP/DFT. Among the DFT functionals, basing on the results previously reported, we used

B3PW91, CAM-B3LYP, PBE0, B97-1 and the popular B3LYP one. Concerning the calculations of the cubic force field, for CH_2ClF we employed the AVTZ basis set, while for $ClFC=CH_2$ we chosen the VTZ-AVTZ(F) one. For comparison purposes, we used the B3LYP functional also in conjunction with the double-zeta SNSD and N07D basis set. Table 5 reports the results obtained for CH_2ClF, while the corresponding data for $ClFC=CH_2$ are listed in Table 6. From the inspection of both the Tables, the overall good performances of B3PW91, CAM-B3LYP, PBE0 and B97-1 are further confirmed.

4. Conclusions

In the present work we investigated the performances of different DFT methods for the calculations of sextic centrifugal distortion constants with respect to the results obtained at HF-SCF, MP2, CCSD and CCSD(T) level of theory. From this analysis, we can highlight the following points.

- The MP2 level of theory in conjunction with triple-zeta basis set augmented by diffuse functions predicts values in good agreement with those obtained at CCSD(T) level of theory.
- At DFT level of theory, PBE0, CAM-B3LYP, B97-1, B2PLYP and B3PW91 on average yield good results in conjunction with almost all the basis sets considered.
- Within the framework of DFT methods, even if there is a slight increase in the overall performances when going from AVTZ to AVQZ basis sets, the former seems to be the right tradeoff between reliable results and computational costs.
- The use of an hybrid approach where the quadratic part is obtained at CCSD(T) level of theory and the DFT*s* are employed to compute only the cubic force constants yields a dramatic improvement of the overall performances. The best results are obtained by using the B3PW91, CAM-B3LYP, B2PLYP, PBE0 and B97-1 functionals.
- Within the framework of hybrid approach, as a valid alternative (and computationally much less demanding) to that mentioned above, we highlight the use of B2PLYP functional to compute the harmonic parts.

Approaches based on hybrid force fields led to results in excellent agreement to those given by calculations having also the cubic part computed by CCSD(T). Given the small set of molecules here investigated we cannot warrant a straightforward application of these results to more complex

systems and therefore an extension of this study is currently underway. Besides, given the good performances demonstrated by the hybrid approaches carried out in the present investigation, future work will be aimed to check their validity (especially of the B2PLYP/DFT one that can be employed on bigger molecules). Another important issue that in the last years was investigated [87–90] is related to the use of different basis sets in conjunction with DFT methods for computing the Kohn-Sham complete basis set limit (KS-CBS) for several vibrational properties. Recently [91] it was reported that, in conjunction with the B3LYP functional, some basis sets show an irregular behavior, while the newly developed Jensen's polarization consistent pcseg-*n* and aug-pcseg-*n* ones [92] yield smooth and regular trends. Given also their reduced computational cost with respect to the Dunning's correlation consistent basis sets, in the future it would be therefore interesting to test their performances in conjunction with different DFT methods.

Acknowledgments

Financial supports by MIUR (PRIN 2012 funds for project "STAR: Spectroscopic and computational Techniques for Astrophysical and atmospheric Research", prot. no. 20129ZFHFE_003) and by University Ca' Foscari Venezia (ADIR funds) are gratefully acknowledged. The High Performance Computing department of the CINECA Supercomputer Centre (Grant No. HP10C292PO) and the SCSCF ("Sistema per il Calcolo Scientifico di Ca' Foscari", a multiprocessor cluster system owned by Universita' Ca' Foscari Venezia) facilities are gratefully acknowledged for the utilization of computer resources.

Appendix A. Supplementary material

Supplementary data associated with this article can be found, in the online version, at …

References

[1] V. Barone, Ed., in *Computational Strategies for Spectroscopy, from Small Molecules to Nano Systems*, Wiley, Hoboken, New Jersey 2011.

[2] H.H.Nielsen, Rev. Mod. Phys. 23 (1951) 90–136.

[3] G. Amat, H.H. Nielsen, G. Tarrago, Rotation-Vibration of Polyatomic Molecules: New York: Marcel Decker: Amsterdam, 1971.

[4] D. Papoušek, M. R. Aliev, Molecular Vibrational-Rotational Spectra; Elsevier: Amsterdam, 1982.

[5] N. Vogt, J. Vogt, J. Demaison, J. Mol. Struct. 988 (2011) 119–127.

[6] C. Puzzarini, J. F. Stanton, and J. Gauss, Int. Rev. Phys. Chem. 29 (2010) 273–367.

[7] C. Puzzarini, M. Heckert, and J. Gauss, J. Chem. Phys. 128 (2008) 194108.

[8] F. Pawlowski, P. Jørgensen, J. Olsen, F. Hegelund, T. Helgaker, J. Gauss, K. L. Bak, J. Stanton, J. Chem. Phys. 116 (2002) 6482–6496.

[9] N. Vogt, J. Demaison, H. D. Rudolph, Mol. Phys. 112 (2014) 2873–2883.

[10] C. Puzzarini, Int. J. Quant. Chem. 116 (2016) 1513–1519.

[11] E. Penocchio, M. Mendolicchio, N. Tasinato, V. Barone, Can. J. Chem. 94 (2016) 1065–1076.

[12] G. D. Purvis, R. J. Bartlett, J. Chem. Phys.76 (1982) 1910−1918.

[13] K. Raghavachari, G. W. Trucks, J. A. Pople, M. Head-Gordon, Chem. Phys. Lett. 157 (1989) 479–483.

[14] C. Hampel, K.A. Peterson, H.-J. Werner, Chem. Phys. Lett. 190 (1992) 1–12.

[15] M. L. Senent, C. Puzzarini, R. Domínguez-Gómez, M. Carvajal, M. Hochlaf, J. Chem. Phys. 140 (2014) 124302.

[16] T. K. Ormond, A. M. Scheer, M. R. Nimlos, D. J. Robichaud, J. W. Daily, J. F. Stanton, G. B. Ellison, J. Phys. Chem. A 118 (2014) 708–718.

[17] X. Wang, X. Huang, J. M. Bowman, T. J. Lee, J. Chem. Phys. 139 (2013) 224302.

[18]A.D. Becke, J. Chem. Phys. 98 (1993) 5648–5652.

[19]C. Lee, W. Yang, R.G. Parr, Phys. Rev. B 37 (1988) 785–789.

[20] S.H. Vosko, L. Wilk, M. Nusair, Can. J. Phys. 58 (1980) 1200–1211.

[21] P.J. Stephens, F.J. Devlin, C.F. Chabalowski, M.J. Frisch, J. Phys. Chem. 98 (1994) 11623–11627.

[22] M. Piccardo, E. Penocchio, C. Puzzarini, M. Biczysko, V. Barone, J. Phys. Chem. A 119 (2015) 2058–2082.

[23] C. Puzzarini, M. Biczysko, V. Barone, J. Chem. Theory Comput. 6 (2010) 828.

[24] J. Bloino, M. Biczysko, V. Barone, J. Chem. Theory Comput. 8 (2012) 1015.
[25] I. Carnimeo, C. Puzzarini, N. Tasinato, P. Stoppa, A. Pietropolli Charmet, M. Biczysko, C. Cappelli, V. Barone, J. Chem. Phys. 139 (2013) 074310.
[26] A. Pietropolli Charmet, P. Stoppa, N. Tasinato, S. Giorgianni, V. Barone, M. Biczysko, J. Bloino, C. Cappelli, I. Carnimeo, C. Puzzarini, J. Chem. Phys. 139 (2013) 164302.
[27] A. Pietropolli Charmet, P. Stoppa, N. Tasinato, S. Giorgianni, A. Gambi, J. Phys. Chem. A 120 (2016) 8369–8386.
[28] C. Møller, M. S. Plesset, Phys. Rev. 46 (1934) 618−622.
[29] T. H. Jr. Dunning, J. Chem. Phys. 90 (1989) 1007−1023.
[30] D. E. Woon, T. H. Jr. Dunning, J. Chem. Phys. 98 (1993) 1358−1371.
[31] R. A. Kendall, T. H. Jr. Dunning, R.J.Harrison, J. Chem. Phys. 96 (1992) 6796−6806.
[32] Available at http://dreamsnet.sns.it/downloads. Accessed on December 14, 2016.
[33] C. D. Thompson, E. G. Robertson, D. McNaughton, Mol. Phys. 102 (2004) 1987–1695.
[34] S. Albert, S. Baurecker, M. Quack, A. Steinlin, Mol. Phys. 105 (2007) 541–558.
[35] A. Pietropolli Charmet, N.Tasinato, P. Stoppa, A. Baldacci, S.Giorgianni, Mol. Phys. 106 (2008) 1171−1179.
[36] H. O. Leung, M. D. Marshall, A. L. Vasta, N. C. Craig, J. Mol. Spectrosc. 253 (2009) 116−121.
[37] J. Scaranto, P. Stoppa, A. Pietropolli Charmet, S. Giorgianni, Mol. Phys. 107 (2009) 237–244.
[38] D. McNaughton, E. G. Robertson, C. D. Thompson, T. Chimdi, M. K. Bane, D. Appadoo, Anal. Chem. 82 (2010) 7958–7964.
[39] D. C. McKean, M. M. Law, P. Groner, A. R. Conrad, M. J. Tubergen, D. Feller, M. C. Moore, N. C. Craig, J. Phys. Chem. A 114 (2010) 9309–9318.
[40] D. C. McKean, B. van der Veken, W. Herrebout, M. M. Law, M. J. Brenner, D. J. Nemchick, N. C. Craig, J. Phys. Chem. A 114 (2010) 5728−5742.
[41] A. Pietropolli Charmet, P. Stoppa, N. Tasinato, A. Baldan, S. Giorgianni, A. Gambi, J. Chem. Phys. 133 (2010) 044310.
[42] D. Feller, N. C. Craig, P. Groner, D. C. McKean, J. Phys. Chem. A 115 (2011) 94–98.
[43] A. Pietropolli Charmet, N. Tasinato, P. Stoppa, S. Giorgianni, A. Gambi, Mol. Phys. 109 (2011) 2163–2172.
[44] H. O. Leung, M. D. Marshall, A. T. Bozzi, P. M. Cohen, M. Lam, J. Mol. Spectrosc. 267 (2011) 43−49.

[45] G. Cazzoli, L. Cludi, C. Puzzarini, P. Stoppa, A. Pietropolli Charmet, N. Tasinato, A. Baldacci, A. Baldan, S. Giorgianni, R. W. Larsen, S. Stopkkowicz, J. Gauss, J. Phys. Chem. A. 115 (2011) 453–459.

[46] N. Tasinato, P. Stoppa, A. Pietropolli Charmet, S. Giorgianni, A. Gambi, J. Quant. Spectrosc. Radiat. Transfer 113 (2012) 1240–1249.

[47] E. Canè, M. Villa. F.Tamassia, A. Pietropolli Charmet, N.Tasinato, P. Stoppa, S. Giorgianni, Mol. Phys. 112 (2014) 1899–1909.

[48] E. G. Robertson, C. Medcraft, D. McNaughton, D. Appadoo, J. Phys. Chem. A 118 (2014) 10944-10954.

[49] N. Tasinato, G. Regini, P. Stoppa, A. Pietropolli Charmet, A. Gambi, J. Chem. Phys. 136 (2012) 214302.

[50] N. Tasinato, A. Turchetto, P. Stoppa, A. Pietropolli Charmet, S. Giorgianni, J. Chem. Phys. 142 (2015) 134310.

[51] P. Stoppa, N. Tasinato, A. Baldacci, A. Pietropolli Charmet, S. Giorgianni, F. Tamassia, E. Canè, M. Villa, J. Quant. Spectrosc. Radiative Transf. 175 (2016) 8–16.

[52] P. Stoppa, A. Baldacci, A. Pietropolli Charmet, N. Tasinato, S. Giorgianni, E. Cané, G. Nivellini, Mol. Phys. 111 (2013) 525–534.

[53] P. Stoppa, A. Baldacci, N.Tasinato, A. Pietropolli Charmet, S. Giorgianni, F. Tamassia, E. Cané, M. Villa, Mol. Phys. 113 (2015) 3683-3690.

[54] J. Scaranto, A. Pietropolli Charmet, S. Giorgianni, J. Phys. Chem. C 112 (2008) 9443–9447.

[55] R. Locht, D. Dehareng, B. Leyh, Mol. Phys. 112 (2014) 1520−1539.

[56] R. Locht, D. Dehareng, B. Leyh, J. Phys. B: At., Mol. Opt. Phys. 47 (2014) 0851019.

[57] C.-H. Huang, S.-Yi Chou, S.-B. Jang, Y.-C. Lin, C.-E. Li, C.-C. Chen, J.-L. Chang, J. Phys. Chem. A 120 (2016) 1175 – 1183.

[58] N. Tasinato, A. Pietropolli Charmet, P. Stoppa, S. Giorgianni, A. Gambi, Chem. Phys. 397 (2012) 55–64.

[59] Q. Gou, G. Feng, L. Evangelisti, W. Caminati, Angew. Chem. Int. Ed. 52 (2013) 11888−11891.

[60] U. Adhikari, S. Scheiner, Chem. Phys. 440 (2014) 53–63.

[61] N. Tasinato, D. Moro, S. Stoppa, A. Pietropolli Charmet P. Toninello, S. Giorgianni, Appl. Surf. Sci. 353 (2015) 986–994.

[62] Q. Gou, L.Spada, Y.Geboes, W.A. Herrebout, S. Melandri, W. Caminati, Phys. Chem. Chem. Phys. 17 (2015) 7694−7698.

[63] L. Spada, Q. Gou, Y. Geboes, W. A. Herrebout, S. Melandri, W. Caminati, J. Phys. Chem. A 120 (2016) 4939–4943.
[64] J. P. Perdew,Phys. Rev. B, 33 (1986) 8822–24.
[65] J. P. Perdew, Y. Wang, Phys. Rev. B 45 (1992) 13244–49.
[66] C. Adamo, V. Barone, J. Chem. Phys. 110 (1999) 6158–6169.
[67] A. J. Cohen, N. C. Handy, Mol. Phys., 99 (2001) 607–15.
[68] X. Xu, W. A. Goddard III, Proc. Natl. Acad. Sci. USA, 101 (2004) 2673–77.
[69] Y. Zhao, D. G. Truhlar,Theor. Chem. Acc., 120 (2008) 215–41.
[70] F. A. Hamprecht, A. Cohen, D. J. Tozer, N. C. Handy, J. Chem. Phys., 109 (1998) 6264–71.
[71] T. Yanai, D. Tew, N. Handy, Chem. Phys. Lett., 393 (2004) 51–57.
[72] O. A. Vydrov, G. E. Scuseria, J. Chem. Phys., 125 (2006) 234109.
[73] O. A.Vydrov, J. Heyd, A. Krukau, G. E. Scuseria, J. Chem. Phys., 125 (2006) 074106.
[74] O. A. Vydrov, G. E. Scuseria, J. P. Perdew, J. Chem. Phys., 126 (2007) 154109.
[75] J.-D. Chai, M. Head-Gordon, Phys. Chem. Chem. Phys. 10 (2008) 6615–20.
[76] S. Grimme, J. Comp. Chem., 27 (2006) 1787–99.
[77] S. Grimme, J. Chem. Phys. 124 (2006)034108.
[78] W. Schneider, W. Thiel, Chem. Phys. Lett. 157(1989) 367–373.
[79] M. R. Aliev, J. K. G. Watson, J. Mol. Spectrosc. 61 (1976) 29–52 .
[80] M. R. Aliev and J. K. G. Watson, in Molecular Spectroscopy: Modern Research, Vol. III, edited by K. N. Rao, (Academic Press, New York, 1985) p. 1.
[81] J. K. G. Watson in Vibrational Spectra and Structure, Vol.6, edited by J. During (Elsevier, Amsterdam, 1977) p.1.
[82] J. K. G. Watson, J. Mol. Spectrosc. 65 (1977) 123–133 .
[83] M. J. Frisch, G. W. Trucks, H. B. Schlegel, G. E. Scuseria, M. A. Robb, J. R. Cheeseman, G. Scalmani, V. Barone, B. Mennucci, G. A. Petersson, H. Nakatsuji, M. Caricato, X. Li, H. P. Hratchian, A. F. Izmaylov, J. Bloino, G. Zheng, J. L. Sonnenberg, M. Hada, M. Ehara, K. Toyota, R. Fukuda, J. Hasegawa, M. Ishida, T. Nakajima, Y. Honda, O. Kitao, H. Nakai, T. Vreven, J. A. Montgomery, Jr., J. E. Peralta, F. Ogliaro, M. Bearpark, J. J. Heyd, E. Brothers, K. N. Kudin, V. N. Staroverov, R. Kobayashi, J. Normand, K. Raghavachari, A. Rendell, J. C. Burant, S. S. Iyengar, J. Tomasi, M. Cossi, N. Rega, J. M. Millam, M. Klene, J. E. Knox, J. B. Cross, V. Bakken, C. Adamo, J. Jaramillo, R. Gomperts, R. E. Stratmann, O. Yazyev, A. J. Austin, R. Cammi, C. Pomelli, J. W. Ochterski, R. L. Martin, K. Morokuma, V. G. Zakrzewski, G. A. Voth, P. Salvador, J. J. Dannenberg, S. Dapprich, A. D. Daniels, Ö. Farkas, J. B. Foresman, J. V. Ortiz, J. Cioslowski, and D. J. Fox, Gaussian 09, Revision D.01, Gaussian, Inc., Wallingford, CT, 2009.

[84] CFOUR, Coupled-Cluster techniques for Computational Chemistry, a quantum-chemical program package by J. F. Stanton, J. Gauss, M.E.Harding, et al., and the integral packages MOLECULE (J. Almlöf, P. R. Taylor), PROPS (P.R. Taylor), ABACUS (T. Helgaker, H. J. Aa. Jensen, P. Jørgensen, and J. Olsen), and ECP routines by A. V. Mitin, and C. Wüllen. For the current version, seehttp://www.cfour.de.

[85] A. Pietropolli Charmet, G. Quartarone, L. Ronchin, A. Vavasori, J. Phys. Chem. A 117 (2013) 6846–6858.

[86] C. Puzzarini, G. Cazzoli, J. Gauss, J. Chem. Phys. 137 (2012) 154311.

[87] A. Buczek, T. Kupka, M. A. Broda, J. Mol. Model. 17 (2011) 2029–2040.

[88] A. Buczek, T. Kupka, M. A. Broda, J. Mol. Model. 17 (2011) 2265–2274.

[89] A. Buczek, T. Kupka, S. P. A. Sauer, M. A. Broda, J. Mol. Model. 18 (2012) 2471–2478.

[90] M. A. Broda, A. Buczek, T. Kupka, J. Kaminsky, Vibr. Spectrosc. 63 (2012) 432–439.

[91] A. Buczek, T. Kupka, M. A. Broda, A. Zyla, J. Mol. Model. 22 (2016) 42.

[92] F. Jensen, J. Chem. Theory Comput. 10 (2014) 1074–1085.

Figure Captions

Figure 1. Performances, expressed in term of mean absolute percentage deviation, MAD, with respect to the best computed data in the literature for CH_2F_2 of the different DFT methods in conjunction with AVDZ, AVTZ and AVQZ basis sets.

Figure 2. Performances, expressed in term of mean absolute percentage deviation, MAD, with respect to the best computed data in the literature for $CH_2{}^{35}ClF$ of the different DFT methods in conjunction with AVDZ, AVTZ and AVQZ basis sets.

Figure 3. Performances of different hybrid force fields (set CCSD/DFT) sorted according to their mean absolute percentage deviation, MAD, with respect to the data obtained at CCSD/AVTZ level of theory for $CH_2{}^{35}ClF$. For each hybrid force field its maximum absolute percentage deviation, MAX, is also reported.

Figure 4. Performances of different hybrid force fields (set CCSD(T)/DFT) sorted according to their mean absolute percentage deviation, MAD, with respect to the data obtained at CCSD(T)/AVTZ level of theory for $CH_2{}^{35}ClF$. For each hybrid force field its maximum absolute percentage deviation, MAX, is also reported.

Figure 5. Performances of different hybrid force fields (set CCSD/DFT) sorted according to their mean absolute percentage deviation, MAD, with respect to the computed data of $CH_2{}^{35}ClF$ reported in the literature. For each hybrid force field its maximum absolute percentage deviation, MAX, is also reported.

Figure 6. Performances of different hybrid force fields (set CCSD(T)/DFT) sorted according to their mean absolute percentage deviation, MAD, with respect to the computed data of $CH_2{}^{35}ClF$ reported in the literature. For each hybrid force field its maximum absolute percentage deviation, MAX, is also reported.

Figure 7. Performances of different hybrid force fields (set CCSD(T)/DFT) sorted according to their mean absolute percentage deviation, MAD, with respect to the computed data of $^{35}ClFC{=}CH_2$ reported in the literature. For each hybrid force field its maximum absolute percentage deviation, MAX, is also reported.

Table 1. Performances of the DFT functionals in conjunction with different basis sets for CH_2F_2.[a]

		VDZ	VDZ-AVDZ(F)	AVDZ	VTZ	VTZ-AVTZ(F)	AVTZ	VQZ	VQZ-AVQZ(F)	AVQZ	SNSD	N07D
B2PLYP	*MAD*	2.8	7.4	5.3	2.5	3.3	4.1	1.8	2.5	2.5	-	-
	MAX	20.3	19.5	6.6	4.7	7.3	9.0	3.8	4.1	4.2	-	-
B97-1	*MAD*	3.5	6.7	5.1	2.9	3.0	3.6	2.4	2.5	2.6	-	-
	MAX	17.7	15.6	6.6	6.2	7.6	9.6	5.0	4.1	3.7	-	-
B3PW91	*MAD*	4.5	7.2	5.9	1.9	2.0	3.2	3.3	2.6	2.8	-	-
	MAX	16.8	17.7	8.9	4.5	4.3	5.0	4.8	4.9	4.7	-	-
B3LYP	*MAD*	4.4	7.9	6.7	3.4	3.9	4.8	3.1	3.5	3.3	3.7	4.5
	MAX	15.2	19.7	11.2	5.5	5.9	7.5	6.3	6.2	6.3	6.1	6.7
M06	*MAD*	10.1	9.1	5.5	5.3	4.6	5.4	4.3	5.0	4.5	-	-
	MAX	55.9	29.8	18.6	11.3	10.6	11.9	8.1	10.1	9.1	-	-
M06-2X	*MAD*	9.6	4.2	2.8	1.6	1.7	1.9	2.0	1.8	1.9	-	-
	MAX	53.0	17.1	9.8	3.9	4.1	3.8	4.5	3.7	3.7	-	-
O3LYP	*MAD*	3.8	8.5	6.8	3.5	3.8	4.3	5.0	4.1	4.3	-	-
	MAX	16.2	14.7	9.7	7.1	6.9	7.9	7.6	7.5	7.6	-	-
X3LYP	*MAD*	4.1	7.6	6.4	3.1	3.5	4.5	2.8	3.1	2.9	-	-
	MAX	14.9	20.4	11.9	4.8	5.3	7.7	5.4	5.3	5.4	-	-
ωB97XD	*MAD*	5.6	5.2	3.9	2.2	2.3	2.4	1.6	1.8	1.8	-	-
	MAX	19.6	15.2	6.5	4.8	6.2	8.0	5.8	4.2	4.4	-	-
LC-ωPBE	*MAD*	19.7	4.2	4.2	1.7	1.5	1.8	2.9	2.1	2.4	-	-
	MAX	52.8	17.0	11.2	4.9	5.1	4.6	10.1	7.1	8.5	-	-
PBE0	*MAD*	20.6	6.1	4.4	1.1	0.9	2.0	2.0	1.3	1.5	-	-
	MAX	50.3	18.8	9.5	2.4	2.0	4.2	3.4	2.4	2.5	-	-
CAM-B3LYP	*MAD*	21.3	5.8	5.1	1.4	1.6	2.7	2.4	2.2	2.2	-	-
	MAX	53.4	21.5	14.1	3.3	4.5	8.2	4.4	4.9	3.6	-	-
B97-D	*MAD*	19.0	14.9	13.4	8.9	10.0	11.1	8.5	9.5	9.3	-	-
	MAX	56.1	24.8	18.3	13.2	15.0	15.9	15.4	15.6	15.7	-	-

[a]MAD and MAX are the mean absolute percentage deviation and the maximum absolute percentage deviation, respectively, with respect to the computed values taken from the literature [49].

Table 2. Performances of the DFT functionals in conjunction with different basis sets for $CH_2{}^{35}ClF$.[a]

		VDZ	VDZ-AVDZ(F)	AVDZ	VTZ	VTZ-AVTZ(F)	AVTZ	VQZ	VQZ-AVQZ(F)	AVQZ	SNSD	N07D
B2PLYP	*MAD*	6.0	4.3	3.3	4.9	4.4	3.2	3.2	3.2	3.2	-	-
	MAX	13.7	10.3	9.9	6.8	6.5	4.8	6.3	5.2	5.2	-	-
B97-1	*MAD*	6.3	2.7	2.9	4.8	4.0	3.7	3.5	3.2	3.3	-	-
	MAX	10.5	5.0	6.8	8.9	7.7	8.0	8.4	7.9	7.8	-	-
B3PW91	*MAD*	5.6	2.8	3.0	4.4	3.8	3.5	3.8	3.6	3.6	-	-
	MAX	10.8	7.7	5.7	9.5	8.6	8.9	9.3	8.9	8.9	-	-
B3LYP	*MAD*	8.0	5.0	5.1	6.9	6.1	5.2	5.1	5.0	5.0	6.9	6.2
	MAX	14.7	10.9	8.5	10.3	9.0	9.2	9.4	9.0	8.9	9.6	9.8
M06	*MAD*	7.7	16.9	13.4	9.2	8.9	7.9	6.6	6.8	7.2	-	-
	MAX	19.1	42.9	29.0	23.1	23.2	20.4	15.6	16.1	17.2	-	-
M06-2X	*MAD*	7.7	3.8	2.1	1.7	3.2	2.4	3.2	3.5	3.4	-	-
	MAX	16.9	5.8	3.8	2.4	8.5	6.9	7.4	8.2	7.8	-	-
O3LYP	*MAD*	7.7	4.8	4.7	6.5	6.0	5.7	5.7	5.6	5.6	-	-
	MAX	13.9	9.8	7.4	12.6	11.6	11.5	12.6	11.9	12.8	-	-
X3LYP	*MAD*	7.7	4.6	4.7	6.6	5.7	4.9	4.7	4.6	4.4	-	-
	MAX	13.9	10.8	8.1	9.4	8.1	8.3	8.8	8.3	8.2	-	-
ωB97XD	*MAD*	2.7	3.2	1.6	3.3	2.4	3.5	3.6	3.1	3.2	-	-
	MAX	6.8	4.7	2.6	8.6	3.7	6.2	6.9	5.9	6.2	-	-
LC-ωPBE	*MAD*	4.7	5.1	3.0	2.4	2.1	2.4	3.1	3.0	3.0	-	-
	MAX	7.0	9.1	6.7	4.2	3.8	4.1	6.4	5.9	6.4	-	-
PBE0	*MAD*	5.4	4.2	2.6	3.9	3.4	3.2	3.3	3.2	3.2	-	-
	MAX	10.6	9.3	7.7	6.6	5.6	5.9	8.0	7.7	8.4	-	-
CAM-B3LYP	*MAD*	4.5	4.9	2.9	3.4	2.8	2.5	2.6	2.5	2.5	-	-
	MAX	9.9	7.7	7.5	5.9	6.3	4.3	4.0	4.0	3.9	-	-
B97-D	*MAD*	14.2	11.1	10.6	12.7	12.0	9.4	11.2	11.2	9.7	-	-
	MAX	22.2	21.1	15.3	19.7	18.5	18.7	19.2	18.7	18.9	-	-

[a]MAD and MAX are the mean absolute percentage deviation and the maximum absolute percentage deviation, respectively, with respect to the computed values taken from the literature [26].

Table 3. Performances of the DFT functionals in conjunction with different basis sets for $^{35}ClFC=CH_2$.[a]

		VDZ	VDZ-AVDZ(F)	VTZ	VTZ-AVTZ(F)	VQZ	VQZ-AVQZ(F)	SNSD	N07D
B2PLYP	*MAD*	10.2	5.4	4.5	3.5	-	-	-	-
	MAX	15.2	7.2	6.6	4.4	-	-	-	-
B97-1	*MAD*	8.1	4.6	3.0	1.9	3.0	1.9	-	-
	MAX	12.1	6.3	5.9	3.6	5.9	3.6	-	-
B3PW91	*MAD*	6.3	4.6	1.5	1.3	1.6	1.6	-	-
	MAX	8.0	7.5	3.0	4.2	6.4	6.5	-	-
B3LYP	*MAD*	9.8	6.1	5.4	4.1	5.4	4.1	6.3	6.1
	MAX	14.9	8.5	8.6	6.8	8.6	6.8	8.5	9.4
M06	*MAD*	12.7	9.4	4.4	5.7	6.1	6.0	-	-
	MAX	32.7	28.9	8.9	19.4	20.3	20.1	-	-
M06-2X	*MAD*	12.5	6.0	11.1	10.1	9.6	9.6	-	-
	MAX	32.9	8.9	29.2	25.4	23.5	23.4	-	-
O3LYP	*MAD*	6.5	6.1	2.9	3.7	4.2	4.2	-	-
	MAX	8.9	8.9	10.3	13.5	16.2	16.2	-	-
X3LYP	*MAD*	9.8	6.1	5.5	4.2	3.6	3.6	-	-
	MAX	15.5	8.6	8.7	6.6	5.9	5.8	-	-
ωB97XD	*MAD*	9.4	5.7	5.2	3.9	2.7	2.7	-	-
	MAX	13.9	9.8	8.7	6.0	4.9	4.9	-	-
LC-ωPBE	*MAD*	5.1	4.4	4.7	2.2	2.7	2.6	-	-
	MAX	9.0	8.3	9.0	3.9	4.9	4.8	-	-
PBE0	*MAD*	6.1	4.5	0.9	1.5	2.3	2.2	-	-
	MAX	8.5	8.5	2.3	5.0	7.3	7.2	-	-
CAM-B3LYP	*MAD*	8.7	5.1	4.9	3.6	2.9	2.8	-	-
	MAX	14.0	6.8	8.4	5.7	5.2	4.8	-	-
B97-D	*MAD*	21.3	15.8	17.7	16.1	15.6	15.4	-	-
	MAX	51.6	39.9	46.3	42.1	40.7	40.2	-	-

[a]MAD and MAX are the mean absolute percentage deviation and the maximum absolute percentage deviation, respectively, with respect to the computed values taken from the literature [27].

Table 4. Performances of the DFT functionals in conjunction with different basis sets for $F_2C=CF^{35}Cl$.[a]

		VDZ	VDZ-AVDZ(F)	VTZ	VTZ-AVTZ(F)	SNSD	N07D
B2PLYP	*MAD*	5.5	2.5	1.0	2.8	-	-
	MAX	12.2	5.7	2.4	4.2	-	-
B97-1	*MAD*	3.6	5.8	2.1	3.4	-	-
	MAX	6.2	14.0	3.4	6.5	-	-
B3PW91	*MAD*	3.0	5.6	3.3	4.2	-	-
	MAX	5.7	13.2	6.4	8.2	-	-
B3LYP	*MAD*	4.7	3.2	1.5	2.6	6.3	6.1
	MAX	7.7	7.0	2.9	3.9	8.5	9.4
M06	*MAD*	7.7	3.2	6.4	7.3	-	-
	MAX	18.1	7.1	15.6	17.3	-	-
M06-2X	*MAD*	9.8	10.1	3.5	4.7	-	-
	MAX	19.0	13.7	6.1	6.1	-	-
O3LYP	*MAD*	1.2	6.6	3.3	4.4	-	-
	MAX	3.2	15.3	7.8	10.5	-	-
X3LYP	*MAD*	5.1	3.3	1.7	2.8	-	-
	MAX	8.3	6.9	3.2	3.8	-	-
ωB97XD	*MAD*	3.6	11.1	4.8	5.9	-	-
	MAX	8.7	28.1	11.4	14.4	-	-
LC-ωPBE	*MAD*	4.1	5.1	2.5	3.4	-	-
	MAX	7.4	13.7	5.5	8.1	-	-
PBE0	*MAD*	4.0	6.0	3.7	4.7	-	-
	MAX	7.4	13.4	6.2	8.6	-	-
CAM-B3LYP	*MAD*	5.9	4.4	2.7	3.6	-	-
	MAX	9.8	8.2	4.7	4.9	-	-
B97-D	*MAD*	12.8	7.7	7.0	6.5	-	-
	MAX	30.9	19.3	11.6	11.0	-	-

[a]MAD and MAX are the mean absolute percentage deviation and the maximum absolute percentage deviation, respectively, with respect to the computed values taken from the literature [58].

Table 5. Results (in Hz) of the hybrid force fields (belonging to the B2PLYP/DFT set) for $CH_2{}^{35}ClF$, with respect to computed reference data taken from the literature.[a] Each hybrid force fieldhas the cubic force constants obtained by the DFT listed in the corresponding columns and in conjunction with the AVTZ basis sets, except B3LYP-1 and B3LYP-2, which have SNSD and N07D, respectively.

	B3LYP-1	B3LYP-2	B3LYP	CAM-B3LYP	B3PW91	B97-1	PBE0
$\Phi_J x10^3$	2.703	2.692	2.731	2.932	2.907	2.971	2.982
$\Phi_{JK} x10^2$	4.483	4.374	4.273	4.151	3.974	4.223	3.975
Φ_{KJ}	-2.899	-2.891	-2.863	-2.890	-2.867	-2.879	-2.887
$\Phi_K x10$	2.658	2.652	2.643	2.653	2.650	2.653	2.658
$\phi_J x10^3$	1.056	1.059	1.069	1.102	1.103	1.107	1.114
$\phi_{JK} x10^2$	1.803	1.810	1.855	1.950	1.940	2.020	1.979
ϕ_K	3.277	3.280	3.289	3.289	3.293	3.297	3.292
MAD	6.0	5.5	4.4	2.2	2.6	3.0	2.9
MAX	8.6	7.9	6.6	5.7	5.6	5.7	5.9

[a]MAD and MAX are the mean absolute percentage deviation and the maximum absolute percentage deviation, respectively, with respect to the computed values taken from the literature [26].

Table 6. Results (in Hz) of the hybrid force fields (belonging to the B2PLYP/DFT set) for $^{35}ClFC=CH_2$, with respect to computed reference data taken from the literature.[a] Each hybrid force field has the cubic force constants obtained by the DFT listed in the corresponding columns and in conjunction with the VTZ-AVTZ(F) basis sets, except B3LYP-1 and B3LYP-2, which have SNSD and N07D, respectively.

	B3LYP-1	B3LYP-2	B3LYP	CAM-B3LYP	B3PW91	B97-1	PBE0
$\Phi_J \times 10^4$	7.817	7.755	7.649	8.350	8.115	8.030	8.399
$\Phi_{JK} \times 10^2$	1.421	1.439	1.425	1.417	1.466	1.438	1.475
$\Phi_{KJ} \times 10^2$	-1.328	-1.374	-1.351	-1.283	-1.347	-1.332	-1.338
$\Phi_K \times 10^2$	2.512	2.523	2.513	2.488	2.527	2.537	2.542
$\phi_J \times 10^4$	4.125	4.099	4.050	4.364	4.264	4.208	4.392
$\phi_{JK} \times 10^3$	8.479	8.550	8.438	8.664	8.828	8.616	8.986
$\phi_K \times 10^2$	9.242	9.242	9.228	9.288	9.297	9.261	9.326
MAD	4.8	4.1	5.1	3.3	2.5	3.5	1.6
MAX	7.9	8.6	9.9	8.8	4.4	5.4	4.9

[a]MAD and MAX are the mean absolute percentage deviation and the maximum absolute percentage deviation, respectively, with respect to the computed values taken from the literature [27].

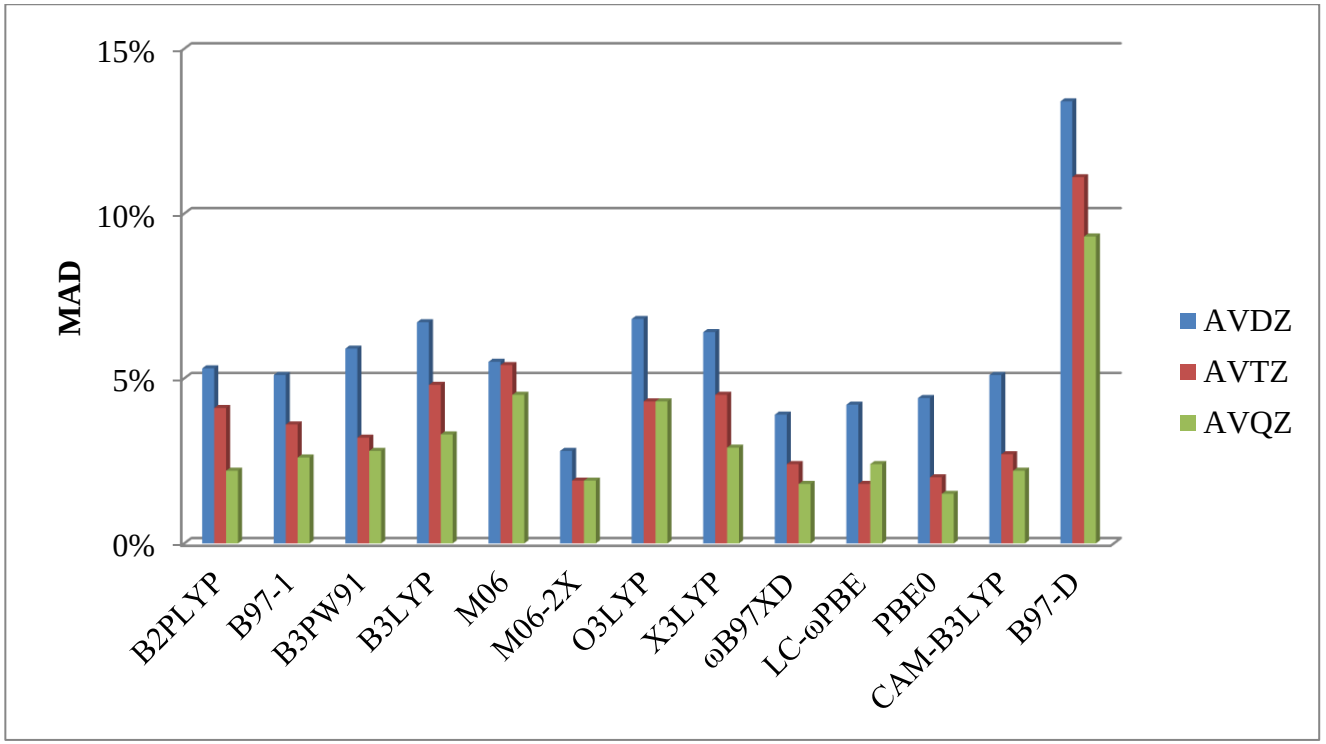
15%
10%
5%
0%
MAD
AVDZ
AVTZ
AVQZ
B2PLYP
B97-1
B3PW91
B3LYP
M06
M06-2X
O3LYP
X3LYP
ωB97XD
LC-ωPBE
PBE0
CAM-B3LYP
B97-D

Figure 1

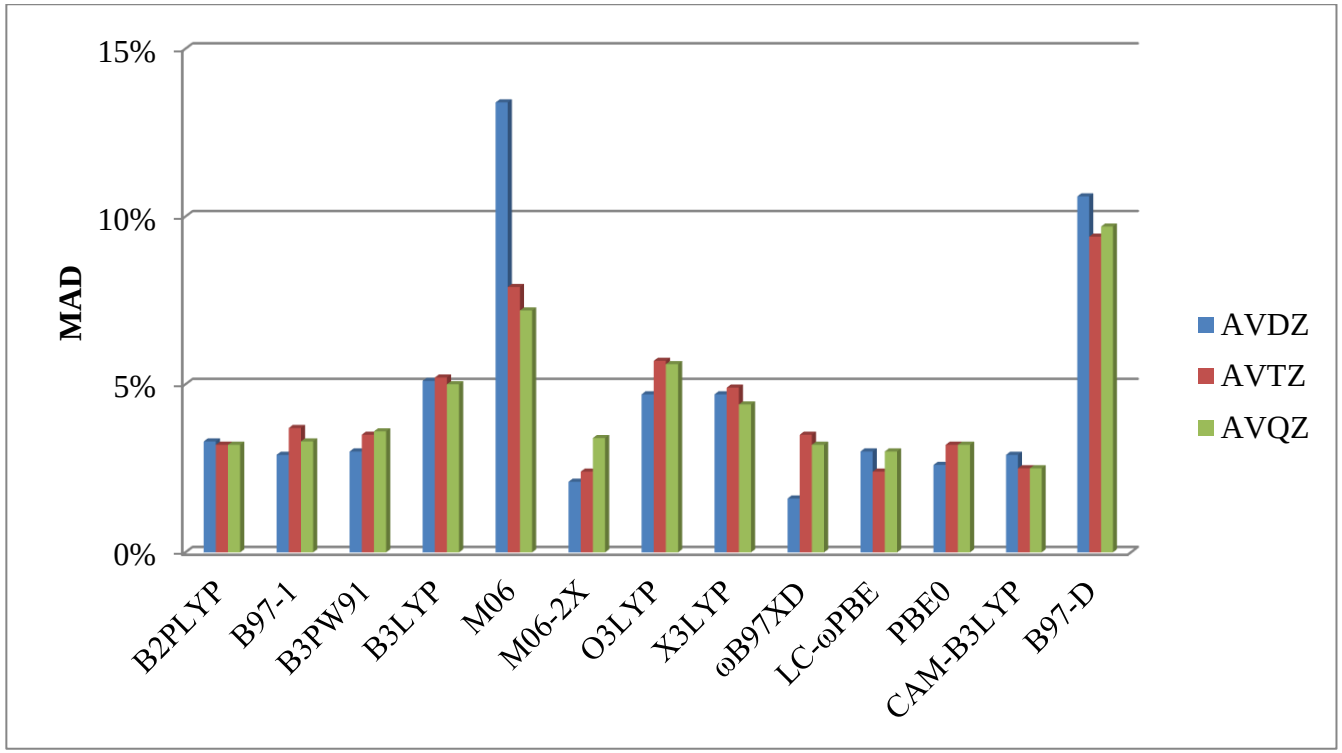
15%
10%
5%
0%
MAD
AVDZ
AVTZ
AVQZ
B2PLYP
B97-1
B3PW91
B3LYP
M06
M06-2X
O3LYP
X3LYP
ωB97XD
LC-ωPBE
PBE0
CAM-B3LYP
B97-D

Figure 2

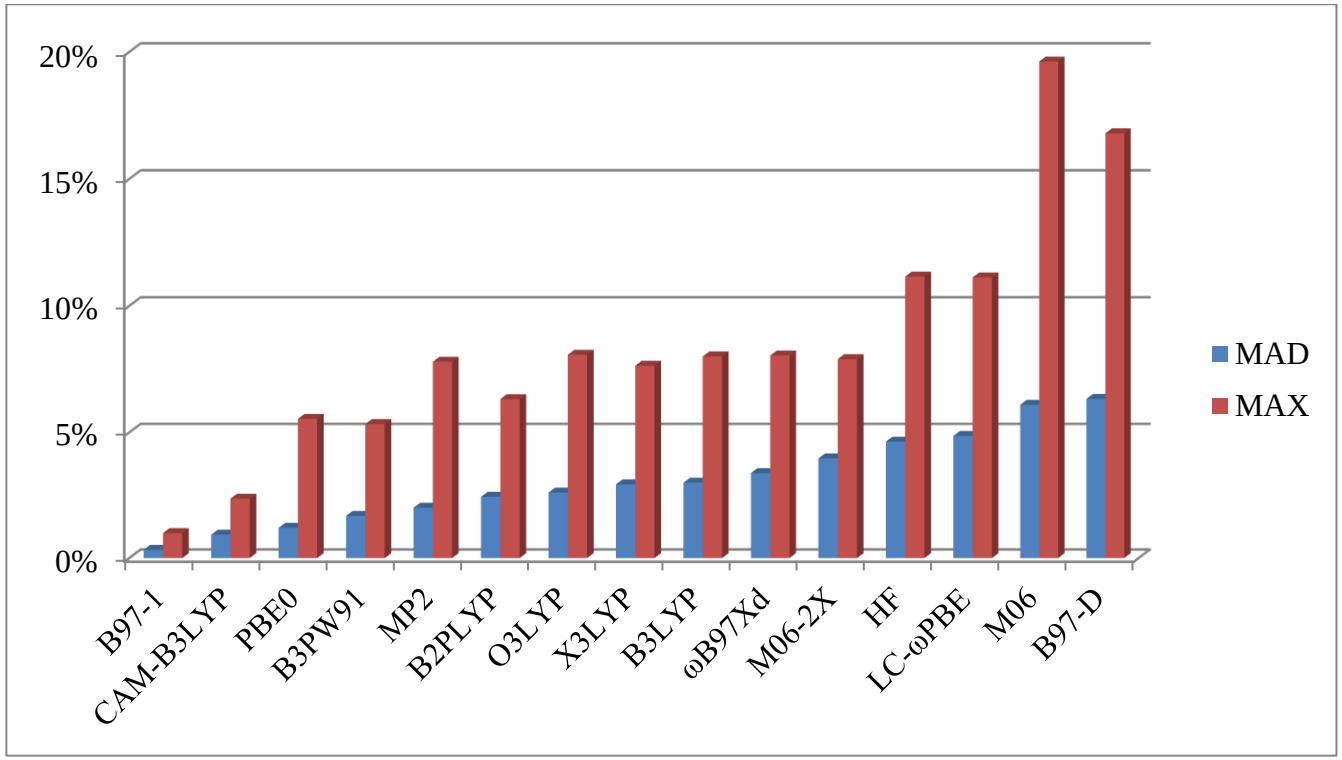
20%
15%
10%
5%
0%
B97-1
CAM-B3LYP
PBE0
B3PW91
MP2
B2PLYP
O3LYP
X3LYP
B3LYP
ωB97Xd
M06-2X
HF
LC-ωPBE
M06
B97-D
MAD
MAX

Figure 3

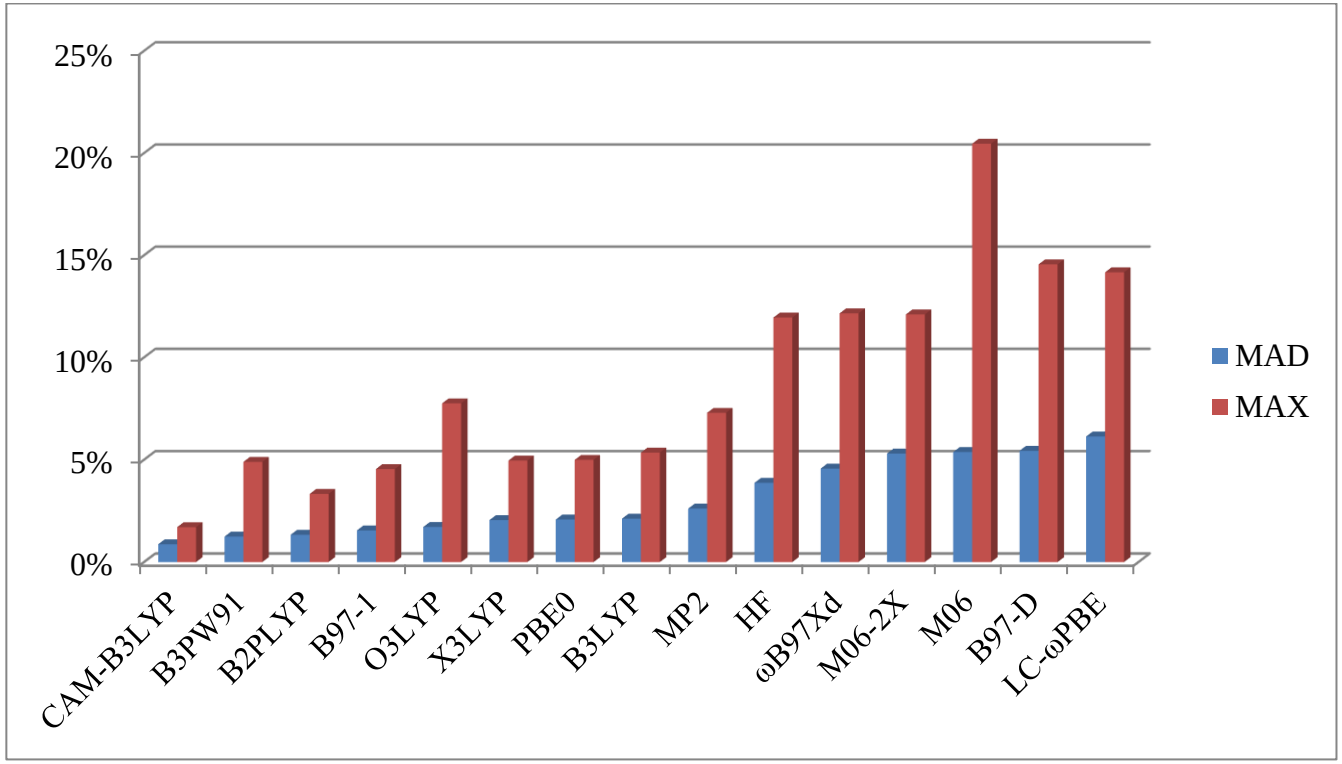
25%
20%
15%
10%
5%
0%
MAD
MAX
CAM-B3LYP
B3PW91
B2PLYP
B97-1
O3LYP
X3LYP
PBE0
B3LYP
MP2
HF
ωB97Xd
M06-2X
M06
B97-D
LC-ωPBE

Figure 4

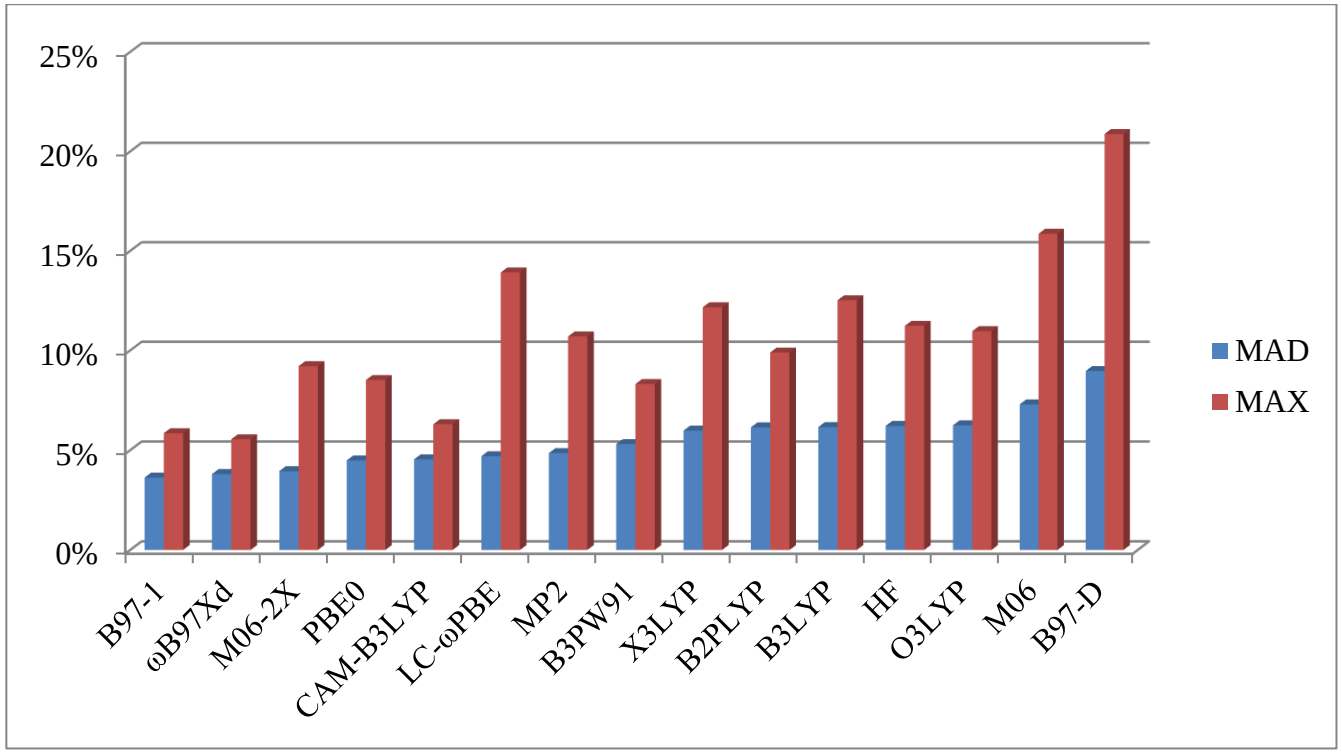
25%
20%
15%
10%
5%
0%
B97-1
ωB97Xd
M06-2X
PBE0
CAM-B3LYP
LC-ωPBE
MP2
B3PW91
X3LYP
B2PLYP
B3LYP
HF
O3LYP
M06
B97-D
MAD
MAX

Figure 5

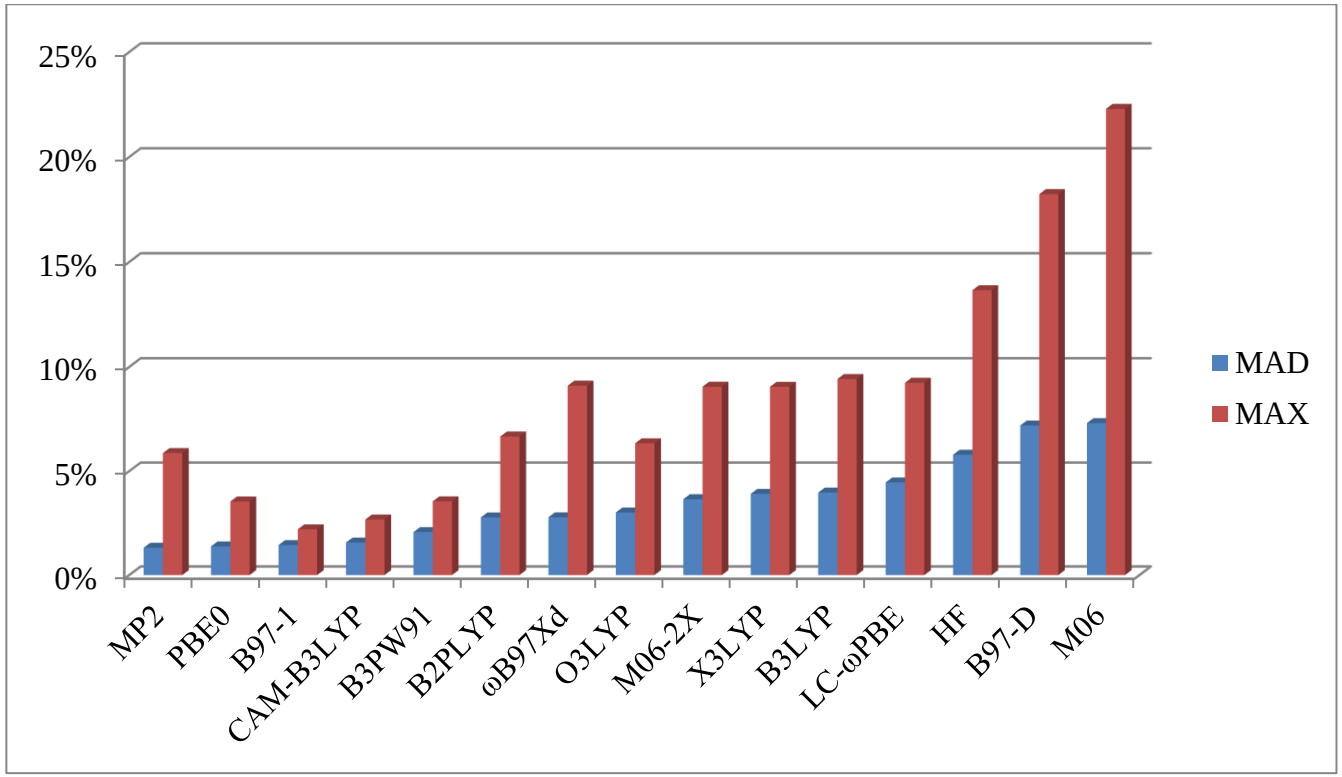
25%
20%
15%
10%
5%
0%
MAD
MAX
MP2
PBE0
B97-1
CAM-B3LYP
B3PW91
B2PLYP
ωB97Xd
O3LYP
M06-2X
X3LYP
B3LYP
LC-ωPBE
HF
B97-D
M06

Figure 6

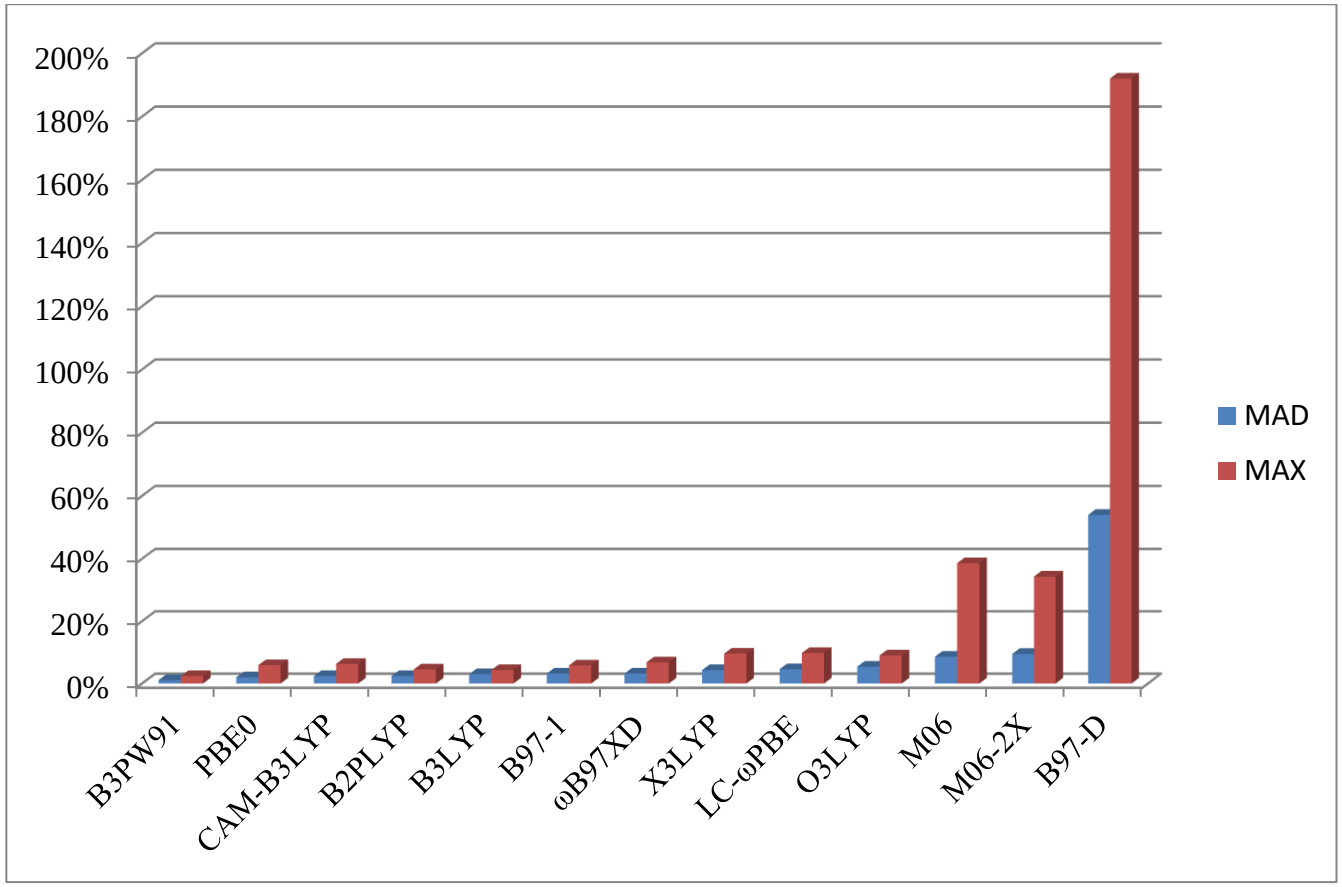
200%
180%
160%
140%
120%
100%
80%
60%
40%
20%
0%
B3PW91
PBE0
CAM-B3LYP
B2PLYP
B3LYP
B97-1
ωB97XD
X3LYP
LC-ωPBE
O3LYP
M06
M06-2X
B97-D
MAD
MAX

Figure 7